Aerosol and Air Quality Research, 17: 644–652, 2017

ISSN: 1680-8584 print / 2071-1409 online
doi: 10.4209/aaqr.2016.07.0293

Development of a Sharp-Cut Inertial Filter Combined with an Impactor

Tong Zhang[1], Hideaki Takahashi[1], Mitsuhiko Hata[2], Akira Toriba[3], Takuji Ikeda[4], Yoshio Otani[2], Masami Furuuchi[2*]

[1] *Graduate School of Natural Science & Technology, Kanazawa University, Kanazawa, 920-1192, Japan*
[2] *College of Science and Engineering, Kanazawa University, Kanazawa, 920-1192, Japan*
[3] *College of Medical, Pharmaceutical and Health Sciences, Kanazawa University, Kanazawa, 920-1192, Japan*
[4] *NITTA CORPORATION, Osaka, 556-0022, Japan*

ABSTRACT

A layered mesh inertial filter that was previously developed by the authors, was combined with an impactor, in which the collection efficiency curve overlaps that of the inertial filter, in order to provide a sharp-cut separation tool for aerosol nanoparticles operating at a moderate pressure drop of less than 10–15 kPa. The separation performance of the proposed "hybrid inertial filter" of the inertial filter and an impactor, such as cut-off size, steepness of the collection efficiency curve and pressure drop ΔP, was evaluated for a single nozzle type in order to confirm the proposed system. The performance of the single nozzle type, which can be used as a unit of a multi nozzle type, was compared with that of the previous type layered mesh inertial filter with a stainless steel fiber mat. The hybrid inertial filter was found to have a collection efficiency curve with a much better steepness at less ΔP compared to those of the previous type for particles with the same cut-off size: a cut-off size d_{p50} of 100 nm with steepness d_{p84}/d_{p16} = 1.7, e.g., was obtained at ΔP ~12 kPa while d_{p84}/d_{p16} = 2.4 at ~16 kPa was found for the previous type.

Keywords: Nanoparticle measurement; Impactors; Filtration; Samplers; Ambient; Classification.

INTRODUCTION

Airborne nanoparticles, which are found, not only in the ambient air but also in locations where nanomaterials are produced, have attracted considerable attention in recent years. They can have adverse influences on human health, since they are able to penetrate into the alveolar regions of the lungs (Kreyling *et al.*, 2002; Kashiwada *et al.*, 2006; Kim *et al.*, 2006; Heal *et al.*, 2012). Both the direct and indirect influence of ultrafine or nanoparticles, i.e., ambient nanoparticles on climate change have also been investigated (e.g., Cai *et al.*, 2016).

Analyzing airborne nanoparticles collected by air samplers at various locations is important in terms of detecting emission sources and evaluating health risks based on various chemical components that are contained by them. One of the problems encountered during the sampling of nanoparticles is the loss of semi-volatile components via evaporation. This is a common problem when using conventional types of air samplers that separate particles based on inertial effects, such as a low pressure impactors (LPI) (Hering *et al.*, 1978, 1979) and a nano-Multi Orifice Uniform Deposit Impactor (nano-MOUDI II) (MSP cooperation, 2015). An "inertial filter" was developed by the authors (Otani *et al.*, 2007; Eryu *et al.*, 2009; Furuuchi *et al.*, 2010a, b) to overcome such a difficulty due to a pressure drop. The currently used inertial filter consists of webbed SUS fibers fixed into a circular nozzle with a diameter ranging from 3–5.2 mm using a separable cassette, and has been used for flow rates ranging from 6–40 L min^{-1} (Otani *et al.*, 2007; Furuuchi *et al.*, 2010a, b; Hata *et al.*, 2012, 2013b). An air sampler developed by the authors using a inertial filter for $PM_{0.1}$ is now commercially available (Kanomax, 2016) and a supplemental stage of $PM_{0.1}$ for the Andersen cascade impactor was also developed by the authors (Hata *et al.*, 2012).

To improve the separation performance of the inertial filter, the authors proposed a different geometry, namely, a layered-mesh inertial filter, which consists of screen meshes sandwiched by thin spacing sheets perforated with a circular hole (Thongyen *et al.*, 2015). The layered mesh geometry provides a uniform and reproducible structure for the inertial filter as well as effective inertial separation by the mesh wires that are aligned perpendicular to the direction of flow. A layered mesh inertial filter using TEM grids as wire mesh was used in the case of a small flow rate

* Corresponding author.
Tel.: +81-76-234-4646; Fax: +81-76-234-4644
E-mail address: mfuruch@staff.kanazawa-u.ac.jp

(5–6 L min^{-1}) and was successfully applied to a personal sampler (Thongyen *et al.*, 2015). For a high volume flow rate, a multi nozzle layered mesh inertial filter was developed using screen wire mesh sandwiched between spacers with circular holes so as to be aligned to provide multi nozzles (Hata *et al.*, 2013a). It has been applied to flow rates of 20–30 L min^{-1} for each nozzle, corresponding to a total of ca. 400–550 L min^{-1}. The layered-mesh inertial filter showed good performance when a webbed SUS fiber mat was used as a pre-separator, which reduced the bouncing effect of particles larger than 300 nm (Hata *et al.*, 2013a). However, the characteristics of the inertial filter are rather similar to those of an air filter and the separation curve lacks steepness. Although it depends on a type of a pre-cut separator combined with the inertial filter, the over estimation of mass of particles larger than cut-off diameter is possible, as well as an associated miss evaluation of the chemical characteristics of nanoparticles.

In the present study, taking into account the above difficulties associated with an inertial filter, the layered mesh inertial filter developed by the authors was combined with an impactor, which has a collection efficiency curve that overlaps that of the inertial filter, in order to provide a sharp-cut separation tool for aerosol nanoparticles at moderate pressure drops of less than 10–15 kPa. The separation performance of the proposed "hybrid inertial filter" including cut-off size, steepness of the collection efficiency curve and pressure drop was evaluated for a single nozzle type "hybrid inertial filter" and the results were compared with those for the previously developed layered mesh inertial filter with a stainless steel fiber mat, which has air filter like behaviour.

INERTIAL FILTER

Concept of Inertial Filter

Fig. 1 describes the concept of the inertial filter (Otani *et al.*, 2007). Large particles are collected by a conventional filter via inertial impaction at a high-filtration velocity while small particles are removed by Brownian diffusion, as shown in Fig. 1. The parameter involved in the inertial impaction is the Stokes number (Hinds, 1999):

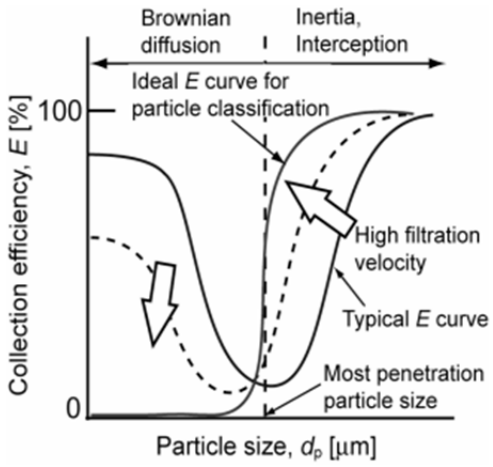

Fig. 1. Principle of inertial filtration.

$$Stk = \frac{C_c \rho_p d_p^2 u}{9 \mu d_f} \quad (1)$$

and the measure for Brownian diffusion is the Peclet number:

$$P_e = \frac{u d_f}{D} \quad (2)$$

where C_c is the Cunningham slip correction factor, ρ_p is the particle density, d_p is the particle diameter, u is the filtration velocity, μ is the viscosity, d_f is the fiber diameter, and D is the Brownian diffusivity of particles. The collection efficiency of a filter increases with increasing *Stk* and decreasing *Pe*. Therefore, an extremely high filtration velocity and a thin fiber would be expected to provide a large inertial effect and a high collection efficiency for larger particles, while the collection efficiency for smaller particles would be low.

Concept of the Hybrid Inertial Filter

Fig. 2 provides information regarding the concept of a hybrid inertial filter. As shown by curve-A in Fig. 2, the collection efficiency curve for the inertial filter shows typical air filter behaviour with a poor steepness of the curve, especially over the 70% region. In order to overcome such difficulty due to the characteristics of the air filter, we propose the use of a combination of a layered mesh inertial filter of cut-off size d_{p50} ~150 nm or slightly larger and an impactor stage of d_{p50} ~200 nm with a steeper separation performance curve that are extensively overlapped with that of the inertial filter (See curve-B in Fig. 2). The curve-C in Fig. 2 represents the performance curve of the combination of an inertial filter and an impactor located just upstream from the inertial filter. Coarse particles bouncing on the inertial filer can be removed by the combined impactor, thus resulting in an increase in the steepness of the total separation curve. In the following discussion, an inertial filter with the combined impactor is referred to as the "hybrid inertial filter". It was designed to provide cut-off size d_{p50} ~100 nm with an improved steepness at a minimal increase in pressure drop, which is sufficiently low to permit it to be used in available portable air samplers. Since the total collection efficiency is increased for the hybrid inertial filter, the inertial filter with d_{p50} larger than 100 nm can provide d_{p50} = 100 nm. This leads to a less pressure drop of the inertial filter.

EXPERIMENTAL

The separation performance of the proposed type inertial filter was tested for single nozzle geometry taking into account the scale up ability shown for the multi-nozzle type using the same nozzle (Hata *et al.*, 2013a). Separation efficiency curves and pressure drop for a layered mesh inertial filter, an impactor and an impactor combined layered mesh inertial filter were compared. For comparison, the previous type of inertial filter combined with a fiber matt was also tested.

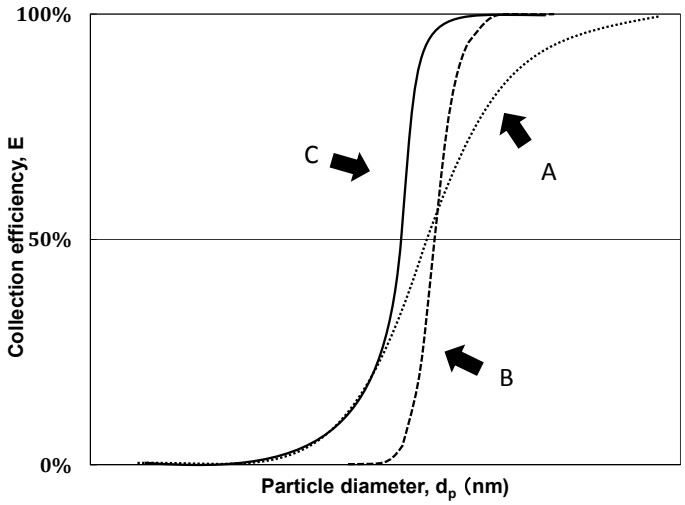

Fig. 2. Concept of the hybrid inertial filter.

Single-Nozzle Inertial Filter

Figs. 3(a)–3(c) show pictures of (a) a circular wire mesh screen (Asada Mesh, SHS-380/114, calendared, ϕ47 mm) (Asada mesh, 2016), (b) a circular spacing sheet (SUS-304, ϕ47 mm, thickness 0.1 mm) with a single circular hole (ϕ3.5 mm) at the sheet center, and (c) a slit nozzle impactor (SKC, Siutas Impactor Stage-D, slit width W = 0.15 mm, nozzle exit to plate distance S = 1.5 mm (S/W = 10), slit length = 20 mm). The wire mesh screen was originally manufactured for screen printing and calendared by roller pressing to provide a mesh thickness almost equivalent to the wire diameter and rigid mesh structure which is important in terms of the re-use of wire meshes. The specifications of the wire mesh screen and spacing sheets are summarized in Tables 1 and 2, respectively. The cut-off size of the slit nozzle impactor, which was originally designed to be 0.25 μm at 9 L min^{-1}, was adjusted for required flow rates by masking the slit by means of a tape to change the nozzle velocity. 5-circular wire mesh screens (a) were sandwiched by 6-spacers (b) and were held tightly in the holder to produce a single nozzle inertial filter. For the uniform layered mesh structure projected in the flow direction (Hata *et al.*, 2013a), wire mesh screens were aligned tangentially uniform in order to maximize the coverage of the nozzle cross section by the mesh wires. The impactor (c) is connected upstream of the filter holder when the performance of the hybrid inertial filter was evaluated. For comparison, the separation performance of the previous type of inertial filter, which uses a stainless fiber mat placed immediately in front of the layered mesh inertial filter in place of the combined impactor, was also evaluated at corresponding experimental conditions. The specifications of the stainless fiber mat are shown in Table 3.

Experimental Setup for the Performance Test and Test Conditions

Fig. 4 shows the setup used for the separation performance test, which consists of the inertial filter holder, the slit impactor connected upstream of the inertial filter, an air pump, a mass flow meter, a mass flow controller, CPC (TSI, Model 3785) connected both upstream and downstream of the filter holder and a system for generating monodispersed aerosol particles. Mono-dispersed zinc chloride ($ZnCl_2$) particles were generated for a test aerosol using an evaporation-condensation type aerosol generator and a TSI-long type DMA. The test aerosol was introduced to the filter holder at selected flow rates after being diluted by clean air. The collection efficiency was determined based on the particle number counted by the CPC. The pressure drop through the inertial filter and the impactor was measured using a digital manometer (EXTECH, Model HD750). The mobility equivalent diameter was converted to an aerodynamic diameter using the density of the test particles as measured by an Aerosol Particle Mass Analyzer (KANOMAX, APM 3600).

For a size range larger than ~100 nm, separation performance was evaluated both by the above described aerosol generating system and ambient aerosol particles. For a poly-dispersed ambient aerosol, a Laser Aerosol Spectrometer (LAS) (TSI, Model 3340) was used for the measurement of particle concentration before and after separation. The aerodynamic diameter by DMA-CPC and the optical diameter from LAS was preliminarily confirmed to be equivalent within an acceptable difference, as described below.

Experimental conditions such as flow velocity were decided both from conditions for the cut-off size d_{p50} = 100 nm (filtration velocity u = 24.6 m s^{-1}) and the pressure drop allowable for commercially available portable air samplers (Shibata Scientific Technology Ltd., HV-500R/F), or, 15–20 kPa (u = 17.0 and 24.6 m s^{-1}). These samplers are planned to be used for a scale up application of the hybrid inertial filter.

RESULTS AND DISCUSSION

Separation Performance of the Layered Mesh Inertial Filter

Figs. 5(a) and 5(b) show the collection efficiency curve for the layered mesh inertial filter at different filtration

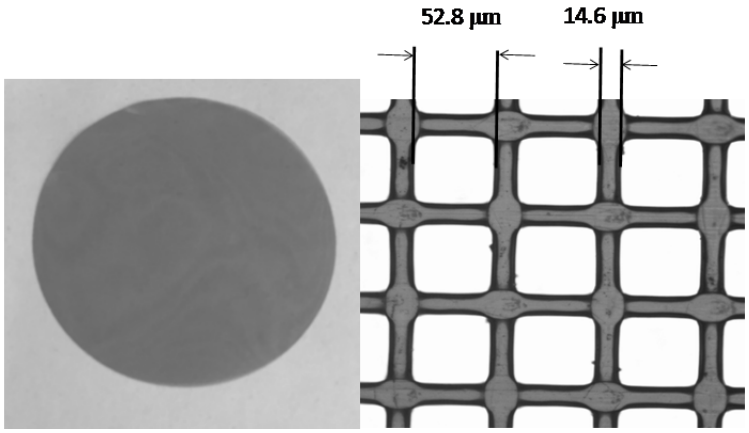

(a)

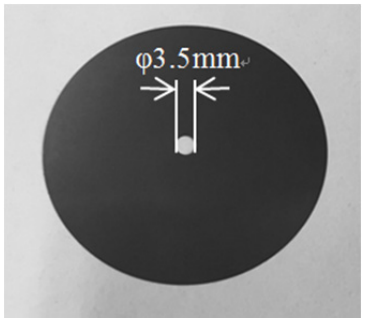

(b)

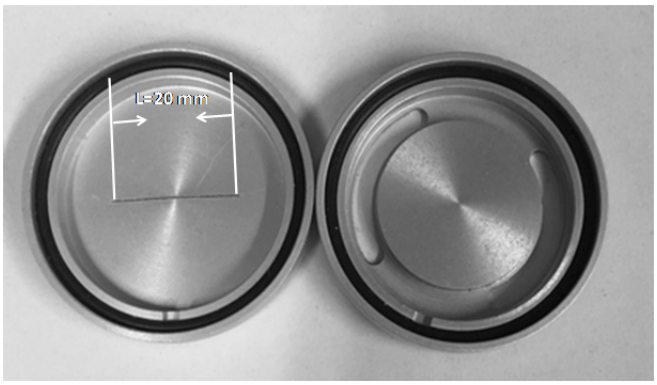

(c)

Fig. 3. Photo of the wire mesh screen, spacing sheet and impactor.

Table 1. Specifications of the wire mesh screen.

Product code	Mesh	Wire diameter (μm)	Mesh opening (μm)	Aperture ratio (%)	Thickness (μm)
SHS-380/14	380	14.7	52.8	62	14 ± 1

Table 2. Specifications of the spacing sheet.

Material code	Diameter (mm)	Diameter of the circular holes (mm)	Thickness (mm)
SUS-304	47	3.5	0.10

Table 3. Specifications of the stainless fiber mat.

Product code	Material	Fiber diameter (μm)	Thickness (mm)	Mass per unit area(g m^{-2})
12-5-1500	SUS-316L	12[a] (13.6)	5	1500

[a] nominal.

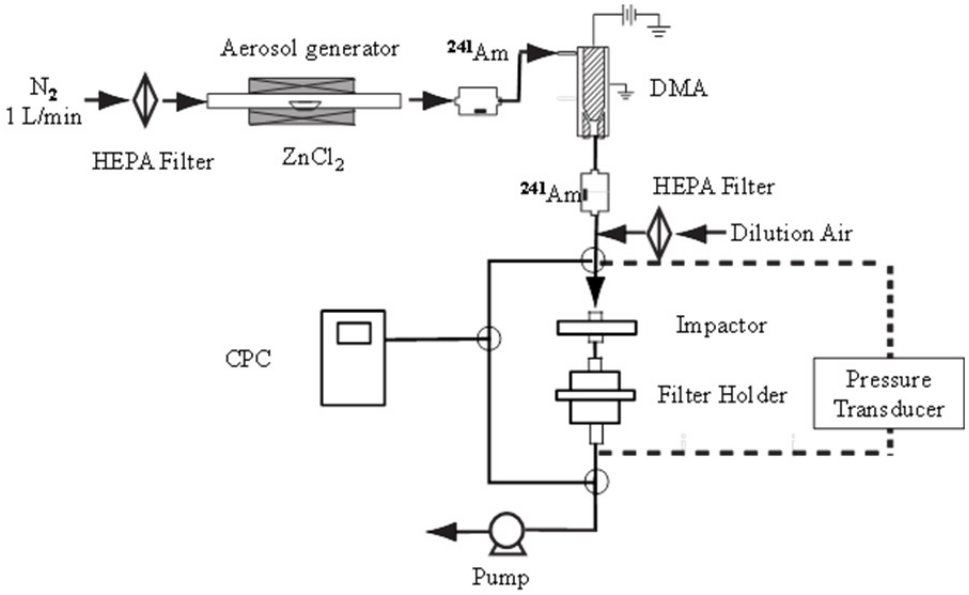

Fig. 4. Schematic diagram of the experimental setup.

velocities u, respectively, at 17.0 and 24.6 m s^{-1}. In both figures, the collection efficiency curve for layered mesh inertial filter combined with a stainless steel fiber matt is shown for comparison. The cut-off size d_{p50} is ~190 nm at u = 17.0 m s^{-1} and the collection efficiency of the layered mesh inertial filter were in good agreement with previous data obtained for ambient particles (Hata *et al.*, 2013a). The collection efficiency of particles larger than ~400 nm decreased due to the bouncing effect at large velocities. Because bouncing was suppressed by the SUS-fiber mat, the collection efficiency of particles of > ~400 nm was improved. This was also confirmed at u = 24.6 m s^{-1} although the bouncing effect started at a slightly smaller size (~300 nm). d_{p50} at u =24.6 m s^{-1} is ~130 nm.

Separation Performance of Impactor

Fig. 6 shows the collection efficiency curves for the impactor that is designed to be combined with the inertial filter for filtration velocities of u = 17.0 and 24.6 L min^{-1}, where the cut-off size d_{p50} ~320 nm at the pressure drop ΔP = 2.9 and 180 nm at ΔP = 4.9 kPa, respectively. The steepness and collection efficiency for coarse particles over 1 μm in diameter are much better than the corresponding values for the inertial filter.

Separation Performance of the Hybrid Inertial Filter

Figs. 7(a) and 7(b), respectively, show collection efficiency curves for the impactor, the layered mesh inertial filter and the hybrid inertial filter at u = 17.0 and 24.6 m s^{-1}. In both figures, the collection efficiency curve for the layered mesh inertial filter with a SUS-fiber mat is shown for comparison, where the curve at u = 24.6 m s^{-1} was obtained in the present experiment. The bouncing effect was suppressed and the separation curve for the hybrid inertial filter was clearly improved. For each filtration velocity, cut-off size d_{p50} = 150 nm at a pressure drop ΔP = 6.4 kPa and 100 nm at ΔP = 11.8 kPa. These pressure drops are still under the allowable pressure drop for the commercial air sampler. Compared to the layered mesh inertial filter with an SUS-fiber mat, the steepness and d_{p50} were improved, although the pressure drop was increased. However, as shown in Fig. 8, for d_{p50} = 100 nm, the pressure drop of the inertial filter with an SUS-fiber mat was larger than that of the hybrid inertial filter while the steepness was much poorer, which cannot be avoided as a characteristic of an "air filter". The cut-off size, pressure drop and steepness of the collection efficiency curves for the hybrid inertial filter at the tested experimental conditions are summarized in Table 4 along with those for the inertial filter with the SUS fiber mat, where the steepness σ of the collection efficiency curve is determined using the following equation (Huang *et al.*, 2005; Tsai *et al.*, 2012):

$$\sigma = \sqrt{\frac{d_{p84}}{d_{p16}}} \tag{3}$$

where d_{p84} and d_{p16} are the particle diameters corresponding to collection efficiencies of 84% and 16%, respectively.

The hybrid inertial filter can provide the same cut-off size with an acceptable steepness of the separation curve at a lower pressure drop than an impactor, although the pressure drop exceeds that of the inertial filter alone.

CONCLUSIONS

The layered mesh inertial filter developed by the authors in a previous study was combined with an impactor, which has a collection efficiency curve that overlaps that of the inertial filter, in order to provide a sharp-cut separation tool for aerosol nanoparticles at moderate pressures. The separation performance of the proposed "hybrid inertial filter" such as cut-off size, steepness of the collection efficiency curve and pressure drop ΔP was evaluated for a

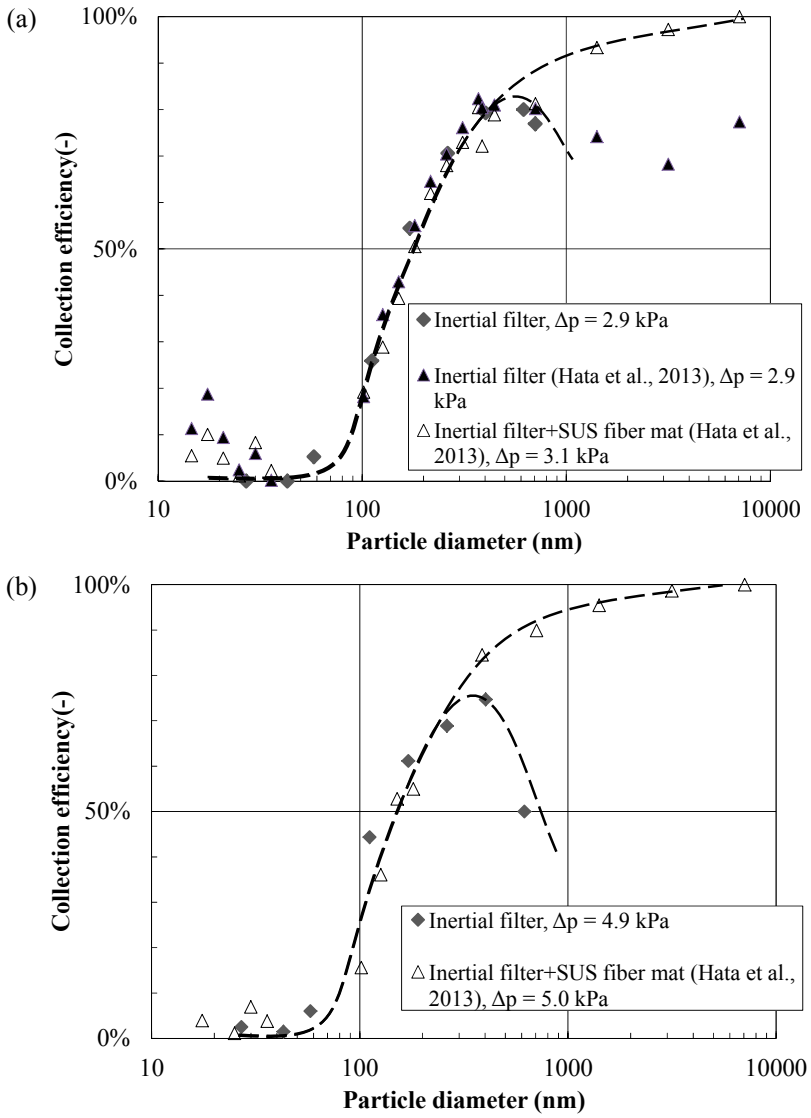

Fig. 5. Collection efficiency curves for the inertial filter.

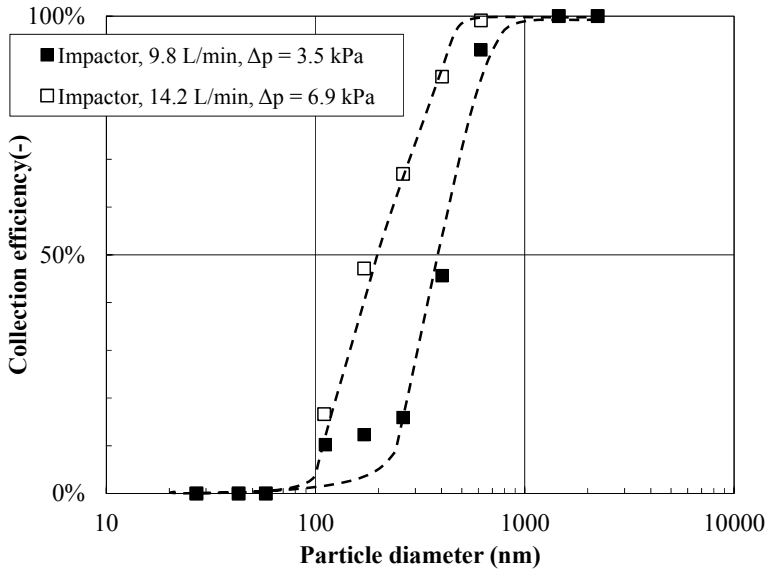

Fig. 6. Collection efficiency curves for the impactor.

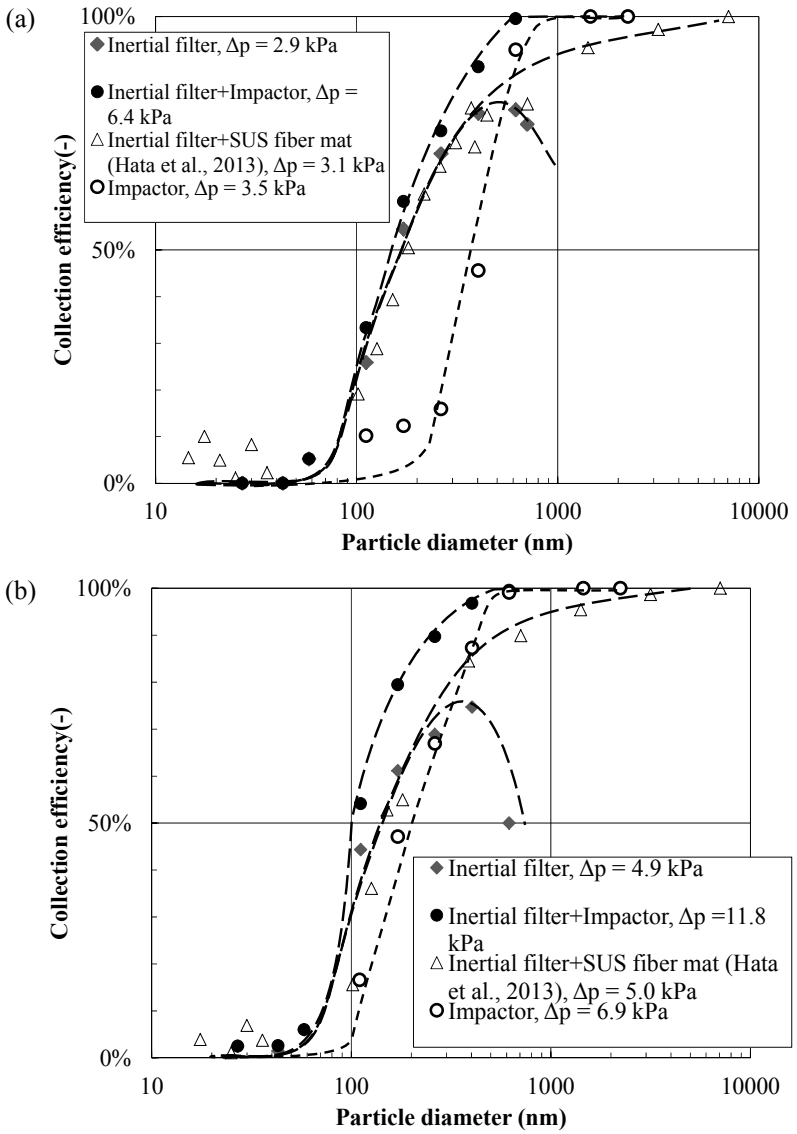

Fig. 7. Collection efficiency curves for the impactor, layered mesh inertial filter and the hybrid inertial filter.

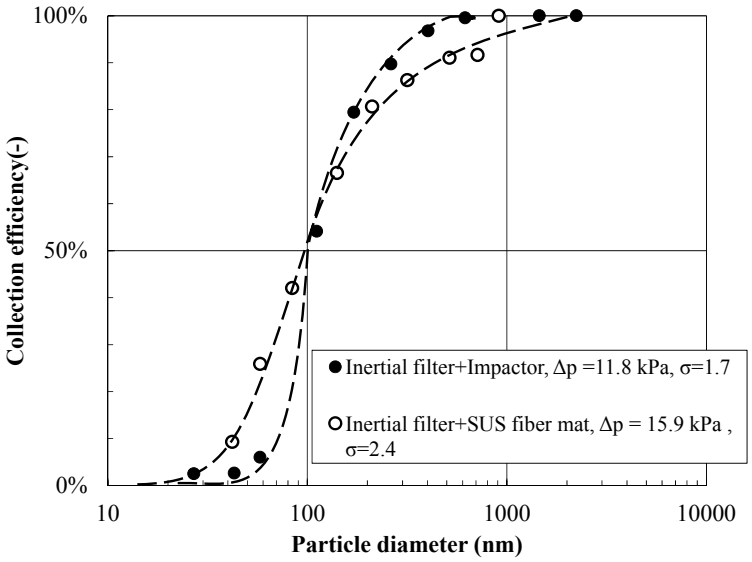

Fig. 8. Collection efficiency curves for the inertial filter with an SUS-fiber mat type and the hybrid inertial filter.

Table 4. Separate performance of the inertial filter with the impactor and SUS fiber mat.

Type	Filtration velocity of inertial filter ($m\ s^{-1}$)	Cut-off size (nm)	Pressure drop ΔP (kPa)	Steepness σ (-)
Inertial filter and impactor	17.0	~150	6.4	1.9
Inertial filter and impactor	24.6	~100	11.8	1.7
Inertial filter and SUS fiber mat	40.7	~100	15.9	2.4
Inertial filter and SUS fiber mat	17.0	~190	3.1	2.3
Inertial filter and SUS fiber mat	24.6	~150	5.0	2.1

single nozzle type "hybrid inertial filter" and compared with that of the previously developed layered mesh inertial filter with a stainless fiber mat. The collection efficiency curve for the hybrid inertial filter showed a much better steepness with a lower ΔP compared to the corresponding values for the previous type at the same cut-off size of particles. A cut-off size of 100 nm with steepness d_{p84}/d_{p16} = 1.7 was obtained at ΔP ~12 kPa while d_{p84}/d_{p16} = 2.4 at ~16 kPa for the previous type. The hybrid structure was shown to overcome a weak point of the inertial filter regarding the bouncing of particles larger than ~300 nm and provided reasonable performance as a sharp-cut tool for nanoparticle separation operated at a moderate pressure drop. This indicates that it can be also applied to coarser cut-off sizes such 200–300 nm with small pressure drops (e.g., < 1–2 kPa). This arrangement has the potential for use in a portable aerosol instrument such as a handheld CPC and other instruments for dealing with ultrafine particles. We are now investigating this possibility. In addition, the hybrid inertial filter can be easily scaled up to a lager flow rate by simply increasing the number of nozzles. We are currently in the process of developing a hybrid inertial filter with a high volume flow rate capacity, which should be applicable for use in commercially available high volume air samplers.

ACKNOWLEDGMENTS

The authors gratefully acknowledge the Japan Promotion for the Promotion of Science (JSPS) for its support of this research (grant No. 15K12185). Also, the authors gratefully acknowledge Shibata Scientific Technology Ltd. for lending us a high volume air sampler and considerable advice regarding this project.

REFERENCES

Cai, C., Xin, Z., Kai, W., Yang, Z., Litao, W., Qiang, Z., Fengkui, D., Kebin, H. and Shao-Cai, Y. (2016). Incorporation of new particle formation and early growth treatments into WRF/Chem: Model improvement, evaluation, and impacts of anthropogenic aerosols over East Asia. *Atmos. Environ.* 124: 262–84.

Eryu, K., Seto, T., Mizukami, Y., Nagura, M., Furuuchi, M., Tajima, Y., Kato, T., Ehara, K., Otani, Y., (2009). Design of inertial filter for classification of $PM_{0.1}$. *J. Aerosol Res.* 24: 24–29 (in Japanese).

Furuuchi, M., Choosong, T., Hata, M., Otani, Y., Tekasakul, P., Takizawa, M. and Nagura, M. (2010a). Development of a personal sampler for evaluating exposure to ultrafine particles. *Aerosol Air Qual. Res.* 10: 30–37.

Furuuchi, M., Eryu, K., Nagura, M., Hata, M., Kato, T., Tajima, N., Sekiguchi, K., Ehara, K., Seto, T. and Otani, Y. (2010b). Development and performance evaluation of air sampler with inertial filter for nanoparticle sampling. *Aerosol Air Qual. Res.* 10: 185–192.

Hata, M., Bao, L. and Furuuchi, M. (2012). Performance evaluation of an andersen cascade impactor with an additional stage for nanoparticle sampling. *Aerosol Air Qual. Res.* 12: 1041–1048.

Hata, M., Thongyen, T., Bao, L., Hoshino, A., Otani, Y., Ikeda, T. and Furuuchi, M. (2013a). Development of a high-volume air sampler for nanoparticles. *Environ. Sci. Processes Impacts* 15: 454–462.

Hata, M., Zhang, T., Bao, L., Otani, Y., Bai, Y. and Furuuchi, M. (2013b). Characteristics of the nanoparticles in a road tunnel. *Aerosol Air Qual. Res.* 10: 185–192.

Heal, M.R., Kumar, P. and Harrison, R.M. (2012). Particles, air quality, policy and health. *Chem. Soc. Rev.* 41: 6606–6630.

Hering, S.V., Flagan, R.C. and Friedlander, S.K. (1978). Design and evaluation of new low-pressure impactor. I. *Environ. Sci. Technol.* 12: 667–673.

Hering, S.V., Friedlander, S.K., Collins, J.J. and Richards, L.W. (1979). Design and evaluation of a new low-pressure impactor. 2. *Environ. Sci. Technol.* 13: 184–188.

Hinds, W.C. (1999). *Aerosol Technology: Properties, Behavior and Measurement of Airborne Particles*, John Wiley & Sons Inc., New York.

Huang, C.H., Chang, C.S., Chang, S.H., Tsai, C.J., Shih, T.S. and Tang, D.T. (2005). Use of porous foam as the substrate of an impactor for respirable aerosol sampling, *J. Aerosol Sci.* 36: 1373–1386

Kashiwada, S. (2006). Distribution of nanoparticles in the see-through medaka (Oryzias latipes). *Environ. Health Perspect.* 114: 1697–1702.

Kim, J.S., Yoon, T.J., Yu, K.N., Kim, B.G., Park, S.J., Kim, H.W., Lee, K.H., Park, S.B., Lee, J.K. and Cho, M.H. (2006). Toxicity and tissue distribution of magnetic nanoparticles in mice. *Toxicol. Sci.* 89: 338–347.

Kreyling, W.G., Semmler, M., Erbe, F., Mayer, P., Takenaka, S., Schulz, H., Oberdörsterb G. and Ziesenis, A. (2002). Translocation of ultrafine insoluble iridium particles from lung epithelium to extrapulmonary organs is size dependent but very low. *J. Toxicol. Environ. Health Part A* 65: 1513–1530.

MSP cooperation (2015). http://www.mspcorp.com/aerosol-instruments/model-122-125-13-stage-moudi-impactors/, Last Access: 30 June 2016.

Otani, Y., Eryu, K., Furuuchi, M., Tajima, N. and Tekasakul, P. (2007). Inertial classification of nanoparticles with fibrous filters. *Aerosol Air Qual. Res.* 7: 343–352.

Thongyen, T., Hata, M., Toriba, A., Ikeda, T., Koyama, H., Otani, Y. and Furuuchi, M. (2015). Development of $PM_{0.1}$ personal sampler for evaluation of personal exposure to aerosol nanoparticles. *Aerosol Air Qual. Res.* 15: 180–187.

Tsai, C.J., Liu, C.N., Hung, S.M., Chen, S.C., Uang, S.N., Cheng, Y.S. and Zhou, Y. (2012). Novel active personal nanoparticle sampler for the exposure assessment of nanoparticles in workplaces. *Environ. Sci. Technol.* 46: 4546–4552.

Received for review, July 20, 2016
Revised, July 20, 2016
Accepted, August 22, 2016